Heliyon 9 (2023) e17714

Contents lists available at ScienceDirect

Heliyon

journal homepage: www.cell.com/heliyon

Vemurafenib induces a noncanonical senescence-associated secretory phenotype in melanoma cells which promotes vemurafenib resistance

Jianyu Peng [a,b,c,†], Zijun Lin [a,b,†], Weichun Chen [a,b], Jie Ruan [b], Fan Deng [d], Lin Yao [a,b], Minla Rao [a,b,1], Xingdong Xiong [a,b], Shun Xu [a,b], Xiangning Zhang [e], Xinguang Liu [a,b,**], Xuerong Sun [a,b,*]

[a] *Guangdong Provincial Key Laboratory of Medical Molecular Diagnostics, The First Dongguan Affiliated Hospital, Guangdong Medical University, Dongguan, 523000, China*
[b] *Institute of Aging Research, School of Medical Technology, Guangdong Medical University, Dongguan, 523000, China*
[c] *Department of Laboratory Medicine, The Third Affiliated Hospital of Guangzhou University of Chinese Medicine, Guangzhou, 510378, China*
[d] *Department of Cell Biology, School of Basic Medical Sciences, Southern Medical University, Guangzhou, 510515, China*
[e] *Department of Pathophysiology, Chinese-American Tumor Institute, Guangdong Provincial Key Laboratory of Medical Molecular Diagnostics, Guangdong Medical University, Dongguan, 523808, China*

ARTICLE INFO

Keywords:
Melanoma
Resistance
Vemurafenib
Cell senescence
Cytokines
BRAF inhibitors

ABSTRACT

More than one half melanoma patients have BRAF gene mutation. BRAF inhibitor vemurafenib is an effective medication for these patients. However, acquired resistance is generally inevitable, the mechanisms of which are not fully understood. Cell senescence and senescence-associated secretory phenotype (SASP) are involved in extensive biological functions. This study was designed to explore the possible role of senescent cells in vemurafenib resistance. The results showed that vemurafenib treatment induced BRAF-mutant but not wild-type melanoma cells into senescence, as manifested by positive β-galactosidase staining, cell cycle arrest, enlarged cellular morphology, and cyclin D1/p-Rb pathway inhibition. However, the senescent cells induced by vemurafenib (SenV) did not display DNA damage response, p53/p21 pathway activation, reactive oxygen species accumulation, decline of mitochondrial membrane potential, or secretion of canonical SASP cytokines. Instead, SenV released other cytokines, including CCL2, TIMP2, and NGFR, to protect normal melanoma cells from growth inhibition upon vemurafenib treatment. Xenograft experiments further confirmed that vemurafenib induced melanoma cells into senescence in vivo. The results suggest that vemurafenib can induce robust senescence in $BRAF^{V600E}$ melanoma cells, leading to the release of resistance-conferring cytokines. Both the senescent cells and the resistant cytokines could be potential targets for tackling vemurafenib resistance.

* Corresponding author. Guangdong Provincial Key Laboratory of Medical Molecular Diagnostics, The First Dongguan Affiliated Hospital, Institute of Aging Research, School of Medical Technology, Guangdong Medical University, Xincheng Avenue 1#, Songshan Lake District, Dongguan 523000, China.

** Corresponding author. Guangdong Provincial Key Laboratory of Medical Molecular Diagnostics, The First Dongguan Affiliated Hospital, Institute of Aging Research, School of Medical Technology, Guangdong Medical University, Xincheng Avenue 1#, Songshan Lake District, Dongguan 523000, China.

E-mail addresses: xgliu@gdmu.edu.cn (X. Liu), xuerongsun@126.com (X. Sun).

† These authors contributed equally to this work and share first authorship.

1 Current addresses: Binhaiwan Central Hospital, Dongguan 532899, China.

https://doi.org/10.1016/j.heliyon.2023.e17714
Received 10 November 2022; Received in revised form 20 June 2023; Accepted 26 June 2023
Available online 3 July 2023

1. Introduction

Malignant melanoma is a lethal skin cancer with rapid metastasis and a poor prognosis. Traditional chemotherapy for melanoma is generally low in effectiveness and high in toxicity. More than half of melanoma patients have a BRAF gene mutation, mostly in the form of BRAFV600E. The BRAF mutation constitutively activates BRAF kinase and the BRAF/MEK/ERK pathway. Targeted therapy with BRAF inhibitors (BRAFi) has been a great breakthrough in melanoma therapy [1,2]. The BRAFi vemurafenib and dabrafenib are highly effective in alleviating symptoms in BRAF-mutant patients [2,3]. Vemurafenib (Vem) was the first FDA-approved BRAFi for melanoma treatment, with a response rate that is very high and efficient. Nevertheless, acquired resistance to BRAFi (including Vem) will inevitably emerge in almost all patients [1,2].

Intensive work has been done to reveal the mechanisms of BRAFi resistance [4–6]. Reactivation of the mitogen-activated protein kinase (MAPK) pathway BRAF/MEK/ERK is one of the key resistance mechanisms. A combination of BRAFi with MEK inhibitors (MEKi) can significantly delay BRAFi resistance and improve therapy outcome [2]. However, such an approach for overcoming BRAFi resistance is still far from ideal.

Cell senescence is a stable cell cycle arrest accompanied by increased senescence-associated β-galactosidase (β-gal) activity, enlarged cellular morphology, activation of the senescence-related pathway, and other functional changes. Senescent cells are metabolically active and generally display an enhanced secretion function, defined as a senescence-associated secretory phenotype (SASP). We reported that the senescent cells and SASP induced by cisplatin (CDDP) underlie drug insensitivity in melanoma cells [7]. BRAFi can also induce cell senescence in melanoma cells [8–10]. However, the role of senescent cells in BRAFi resistance is largely unknown. This study explores the feature of senescent melanoma cells induced by Vem and further investigates the possible role and mechanisms of senescent cells in inducing Vem resistance. Our findings provide new insights into how best to tackle BRAFi resistance.

2. Materials and Methods

2.1. Cell culture and reagents

Melanoma cell lines A375 were purchased from the Type Culture Collection of the Chinese Academy of Sciences in Shanghai, China. Other melanoma cell lines, including A875, M14, MEWO, and MV3, were obtained from iCell Bioscience Inc. In Shanghai, China. The cell lines were authenticated using short tandem repeat (STR) profiling. All the cells were cultured in Dulbecco's Modified Eagle Medium (DMEM, Gibco, CA, USA) with 10% fetal bovine serum (FBS, Hyclone, USA) in a 37 °C humidified incubator. When the cells grew up to 80%–90% confluence, they were routinely passaged into new dishes.

Vemurafenib (S1267) and dabrafenib (S2807) were obtained from Selleck Chemicals, Houston, Texas, USA. The stock solution was rebuilt using dimethyl sulfoxide (D2650; Sigma, St. Louis, Missouri, USA). CDDP (P4394) was obtained from Sigma-Aldrich Co., USA. The cytokine CCL-2 (300–04) was purchased from Thermo Fisher Scientific (USA). TIMP-2 (971-TM-010) and NGFR (367-NR-050) were obtained from R&D System (Minneapolis, MN, USA).

2.2. Detection of β-galactosidase activity

The senescence-associated β-galactosidase (β-gal) staining was performed according to the manual of the kit (C0602; Beyotime Biotechnology, Shanghai, China) [11]. For tumor tissues, cryosections were prepared and fixed. After being incubated with the staining solution at 37 °C overnight, the cells or slices were observed using a microscope equipped with a digital camera (Eclipse TS100; Nikon, Tokyo, Japan).

2.3. Cell proliferation, mitochondrial membrane potential, and reactive oxygen species detection

The integration of 5-Ethynyl-2′-deoxyuridine (EdU) into cell nuclei was employed to evaluate cell proliferation using a Cell-Light EdU Apollo 488 In Vitro Kit (C10310-3, RiboBio Co., Ltd., Guangzhou, China). EdU solution was added to the culture medium to incubate 3 h before cell fixation and staining. Cell fluorescence was observed under a microscope (Olympus, IX73, Japan). A mitochondrial membrane potential (MMP) assay kit with JC-1 (c2006) and a reactive oxygen species (ROS) assay kit (S0033) were purchased from Beyotime Biotechnology and used to assess cellular MMP and ROS accumulation, respectively.

2.4. Conditioned medium collection

The melanoma cells were treated with Vem, CDDP, or vehicle, as indicated in the context. At 24 h before the conditioned medium (CM) harvest, the cells were washed twice with PBS, and the culture dishes were refilled with fresh DMEM medium containing 0.5% FBS with or without Vem. The CM was centrifuged for 10 min at 4 °C, and the supernatant was aliquoted and stored at −80 °C. The cells in each dish were counted. The DMEM medium, which had been kept in a 37 °C incubator for 24 h, was prepared and used to adjust the cell number differences of the various conditioned mediums (CMs).

2.5. Enzyme-linked immunosorbent assay (ELISA)

The CCL2 ELISA kit (DCP00) was a product of R&D Systems. The IL-1α (EK0389), IL-8 (EK0413), and TIMP-2 (EK0522) ELISA kits were provided by Boster Biological Technology, Co. Ltd., China. After dilution of the CM with buffer, the cytokine concentration was detected following the manual of the products. The cell number in each dish was counted and used to adjust the concentration.

2.6. Clone formation assay (CFA)

Normal melanoma cells (A375, M14, or A875) were seeded into culture plates one day before CFA. The various CMs were diluted with fresh DMEM medium (1:1) and added into the wells. Complete DMEM medium acted as the empty control. The cells were cultured under conditions of Vem or vehicle. The medium was refreshed every 3–4 days. When massive clones were observed, the cells were fixed and stained with crystal violet. To quantitatively evaluate the clone density, crystal violet was dissolved using 33% acetic acid, and the optical density (OD) value was detected at 590 nm using a microplate reader. Due to different growth rates, the cells in the Vem- or vehicle-containing medium might be stained at different times.

2.7. Quantitative reverse transcription-PCR (qRT-PCR)

Total RNA of melanoma cells was extracted using TRIzol® Reagent (Life Technologies, USA). PrimeScript™ RT reagent kit containing gDNA Eraser (RR047A, TaKaRa, Japan) was used to synthesize cDNA by reverse transcription reaction. The PCR reaction system was prepared with SYBR™ Select Master Mix (4,472,908, Applied Biosystems, USA), and the reaction volume was 10 μL. The PCR reaction was conducted on a LightCycler® 96 System (Roche, USA). Supplementary Table S1 shows the primer sequences, and GAPDH was used as the reference gene.

2.8. Western blot analysis

Cell pellets were collected and lysed in RIPA buffer containing 50 mM Tris (pH 7.4), 150 mM NaCl, 1% Triton X-100, 1% sodium deoxycholate, 0.1% sodium dodecyl sulfate, and other inhibitors, such as sodium orthovanadate, sodium fluoride, EDTA, and leupeptin. Protein samples were separated using sodium dodecyl sulfate polyacrylamide gel electrophoresis and transferred to polyvinylidene fluoride membranes (Millipore, MA, USA). The membrane was then blocked with 5% milk or 3% bovine serum albumin solution, followed by incubation with primary antibodies at 4 °C. The membranes were then washed three times with TBS containing 0.05% Tween 20 before being incubated with horseradish peroxidase-conjugated secondary antibody. The Azure c400 imaging system (Azure Biosystems, Inc., USA) was used for membrane exposure.

The following antibodies were obtained from Cell Signaling Technology (Beverly, MA, USA), including p-Histone H2A.X (#2577), p53 (#9282 S), p21 (#2946), Akt (pan) (#2920), *p*-Akt (Ser 473) (#9271), p-Rb (Ser 807/811) (#9308), Cyclin D1 (#55506), Erk1/2 (#9102) and *p*-Erk1/2 (Thr202/Tyr204) (#9101). The $p16^{INK4a}$ (ab81278) antibody was obtained from Abcam PLC. (Cambridge, UK) and α-tubulin (T5168) was obtained from Sigma-Aldrich (St. Louis, MO, USA). GAPDH mouse mAb (E1A12400) was purchased from EnoGene Biotech Co., Ltd. (Nanjing, China).

2.9. RNA-seq and data analysis

Melanoma A375 cells were treated with one dose of Vem (10 μM) for 3 days or CDDP (2 μM) for 1 day and then returned to normal culture conditions. On day 7 after the treatment, the cells were collected and lysed with TRIzol® Reagent. Normal cultured A375 cells were used as a negative control. Cells from three independent biological replicates were prepared. RNA-seq and data analysis were performed by BGI Genomics, Shenzhen, China. Briefly, total RNA was extracted from the Trizol lysate. The mRNA was purified using oligo (dT)-attached magnetic beads and further fragmented into small pieces with fragment buffer. After synthesizing the first-strand and second-strand cDNA, the product was amplified by PCR and circularized by the splint oligo sequence to obtain the final library. DNA nanoballs were further obtained and analyzed on an MGIseq2000 platform (BGI, Shenzhen, China). The RNA-seq data have been deposited in NCBI's Gene Expression Omnibus [12] and can be accessed using GEO Series accession number GSE209769.

2.10. In vivo experiments

BALB/c nude mice, male, and aged 4–6 weeks, were purchased from the Center of Experimental Animals, SunYat-sen University, China. All the mice experiments were done following the guidelines for the Animal Ethics Committee of Guangdong Medical University (Approval No. GDY1902028). Considerable efforts were made to minimize the suffering of the mice during the experiments. To obtain melanoma xenografts, A375 cells were subcutaneously injected into the right back of the nude mice. When the average tumor volume reached about 150 mm^3, Vem gavage was performed daily at a dosage of 75 mg/kg for 7 days. Vehicle gavage was administered to the control mice. On day 7 after gavage, the mice were sacrificed, and melanoma tissues were harvested. Cryosections of melanoma tissues were used for β-gal staining and tumor lysates were used for Western blot detection.

2.11. Statistical analysis

The data were calculated and analyzed using SPSS 19 and GraphPad Prism 8.0.1 software. The experimental data are shown as mean ± SD, and the differences of mean were assessed with Student's *t*-test or an analysis of variance. All the results were repeated in at least three independent experiments or samples, except stated otherwise. $P < 0.05$ was considered significant.

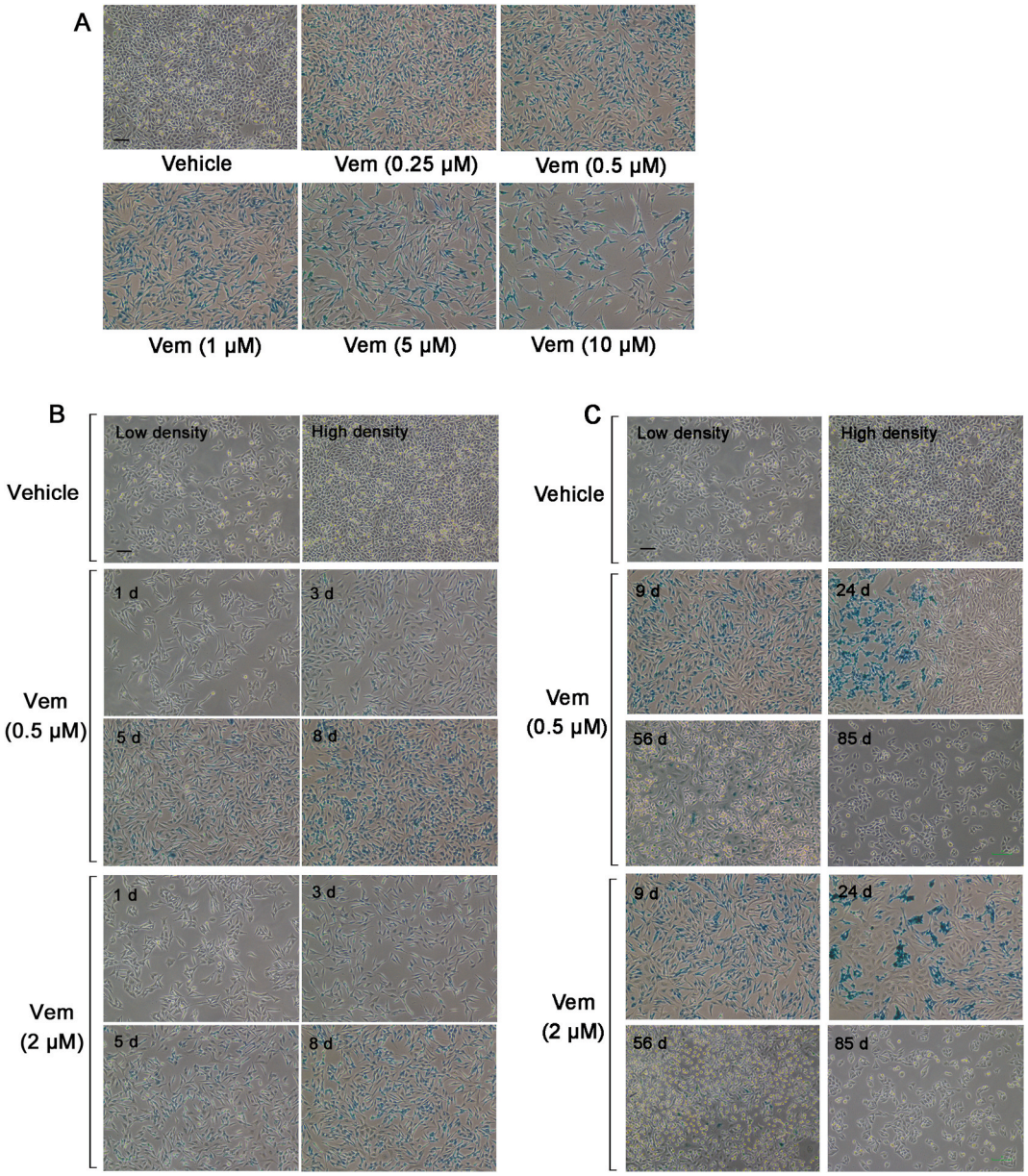

Fig. 1. Continuous vemurafenib treatment enhances β-galactosidase (β-gal) activity in melanoma A375 cells.
A375 cells were continuously treated with vemurafenib (Vem). The day Vem was added was defined as day 0. β-Gal staining was performed at different times. (A) β-Gal staining of A375 cells after 8-day treatment with Vem in various concentrations (0.25 μM–10 μM). The blue-stained cells were positive ones. The vehicle was a solvent control. (B) A375 cells were treated with Vem (0.5 μM or 2 μM) for 1, 3, 5, and 8 days (d) and then stained. The blue color of the stained cells became deeper with time. Few blue-stained cells were observed in the vehicle-treated groups, regardless of the cell density. (C) A375 cells were treated with Vem (0.5 μM or 2 μM) up to 85 days and stained at different time points in an independent experiment. Serial cell passage was firstly initiated on day 24, when cell confluence reached about 90%. The homogeneous cell lines that displayed Vem resistance were observed after about 85 days. Bars are 100 μm.

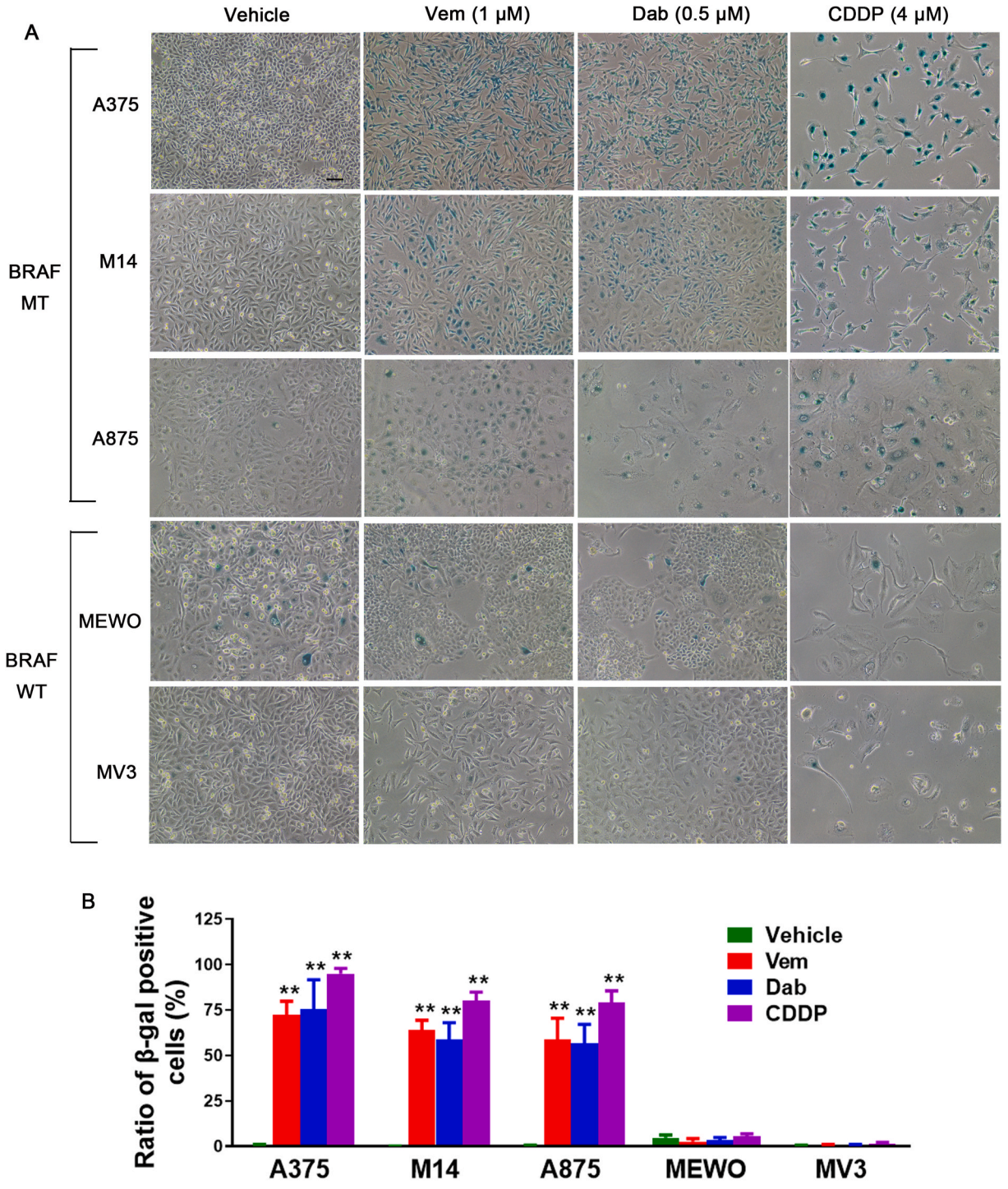

Fig. 2. Continuous treatment with Vem or Dab induces $BRAF^{V600E}$ melanoma cells into β-gal positivity.
BRAF inhibitors Vem and Dab (dabrafenib) were used to treat BRAF mutant (MT) and wild-type (WT) melanoma cell lines continuously for 7 days before β-gal staining. CDDP (cisplatin) treatment was used as a positive control. (A) β-Gal staining of various melanoma cell lines after treatment with Vem, Dab, or CDDP. The vehicle was the solvent control. (B) The statistical ratios of the β-gal positive cells from 3 independent experiments. Bar is 100 μm $^{**}P < 0.01$ *vs.* Vehicle (n = 3).

3. Results

3.1. Continuous treatment with vem induces stable activation of β-gal in melanoma A375 cells

Enhanced β-gal activity is a classical marker of cell senescence [13]. To explore whether Vem could induce melanoma cells into senescence, melanoma A375 cells were treated continuously with Vem of various concentrations (0.25 μM–10 μM). The results showed that Vem inhibited cell proliferation in a concentration-dependent manner. Although some cells detached from the dish bottom, most of the adherent cells became β-gal positive on day 8 after Vem treatment at all concentrations (Fig. 1A).

To evaluate the timeline of cell senescence, β-gal activity was detected continuously in A375 cells after treatment with 0.5 μM or 2 μM Vem. The results showed that the blue-stained cells could be discerned as early as day 3. The color became evident on day 5 and much deeper on day 8 (Fig. 1B). When the treatment was maintained for up to 24 days without cell passage, the color became even deeper, and the blue-stained cells displayed no sign of clonal growth (Fig. 1C). The results implied stable cell cycle arrest in blue-stained cells. After multiple cell passages upon cell confluence, the blue-stained cells gradually decreased and disappeared, and the drug-resistant cell lines with rapid growth were preliminarily established (Fig. 1C).

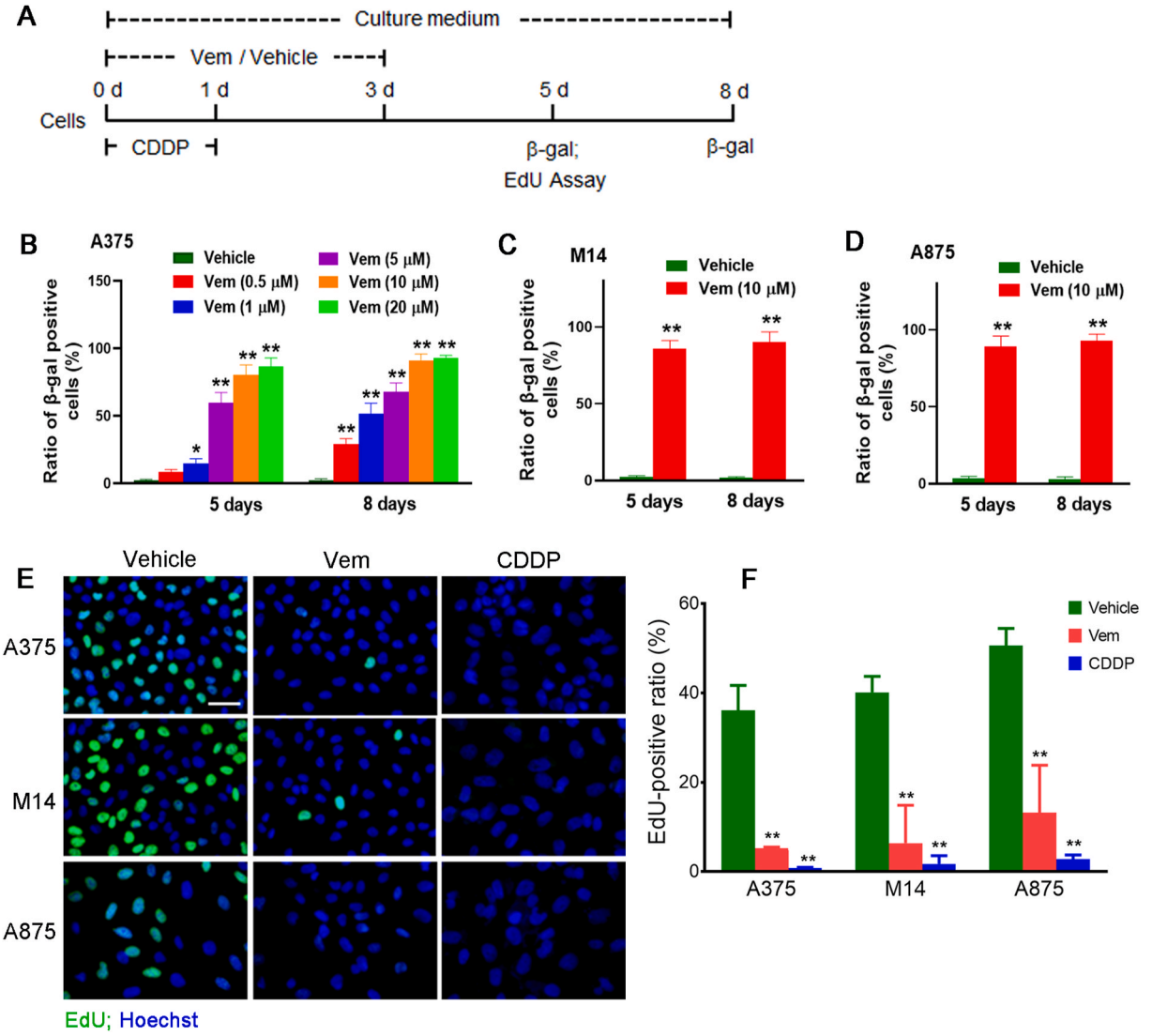

Fig. 3. One dose of Vem treatment induces BRAFV600E melanoma cells into senescence-like cells.
(A) The methods used to treat melanoma cells with one dose of Vem or CDDP. The drugs were removed after 3 days (d) and 1 day, respectively. Detections were performed on day 5 or day 8. (B) The ratio of β-gal positive A375 cells treated once with Vem in various concentrations (0.5 μM–20 μM). (C–D) The ratios of β-gal positive cells in M14 and A875 cells treated with 10 μM Vem. (E–F) Detection of EdU integration in A375, M14, and A875 cells on day 5 after treatment with Vem (10 μM) or CDDP (2 μM). Hoechst was used to stain the nuclei. (F) Positive ratios of EdU integration. *P < 0.05, **P < 0.01 vs. Vehicle (n = 3). The bar is 50 μm.

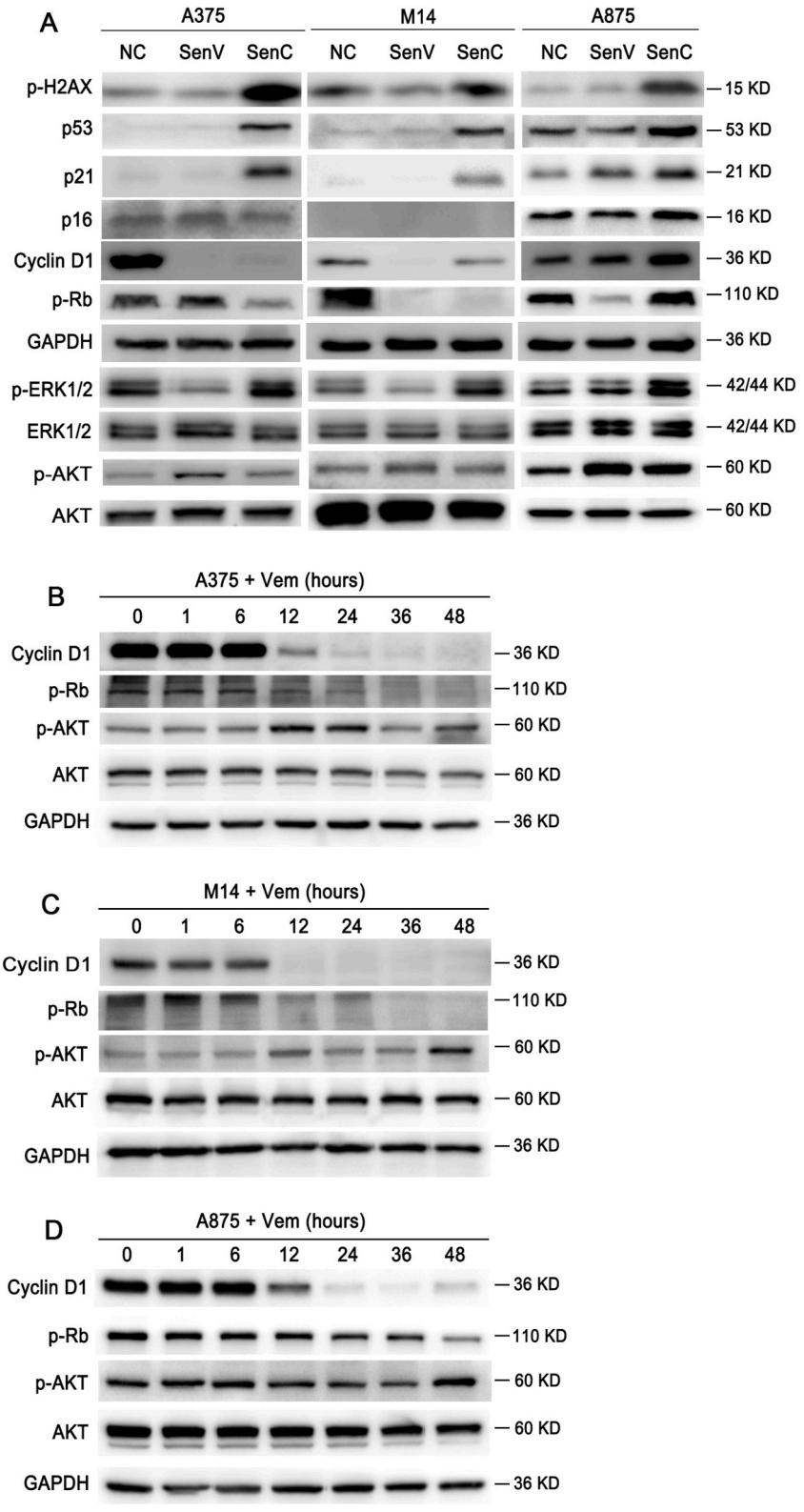

(caption on next page)

Fig. 4. The senescent cells induced by Vem or CDDP display different signal pathway activation.
The senescent cells induced by Vem (SenV) or CDDP (SenC) were obtained on day 5, as shown in Fig. 3A. (A) The expression levels of signal pathway proteins involved in cell senescence or proliferation in SenV and SenC. NC is vehicle control. GAPDH acted as a reference protein. (B-D) The time-dependent effect of Vem (10 μM) on Cyclin D1/p-Rb and AKT pathways during 48-h treatment in A375, M14, and A875 cells, respectively. The unprocessed blot images are presented in Supplementary Fig. S10.

3.2. Vem and dabrafenib specifically enhance β-gal activity in $BRAF^{V600E}$ melanoma cells

Dabrafenib (Dab) is another BRAFi that is frequently used in clinical practice. To further confirm the effect of BRAFi on cell senescence, either Vem or Dab was continuously added to treat melanoma cell lines with or without $BRAF^{V600E}$ mutation. After exposure to Vem or Dab for 8 days, the $BRAF^{V600E}$ cells (i.e., A375, M14, and A875) displayed significant increases in β-gal activity (Fig. 2). By contrast, in the BRAF-wild-type melanoma cell lines MEWO and MV3, neither Vem nor Dab evidently enhanced β-gal activity. CDDP treatment was used as a positive control, as it can induce classical cell senescence in melanoma [7]. Interestingly, CDDP treatment also enhanced β-gal activity in $BRAF^{V600E}$ cells but not in wild-type cells. The results suggest that $BRAF^{V600E}$ melanoma cells were more easily induced into senescence than wild-type cells.

Enlarged cellular morphology is another characteristic of cell senescence [13]. Whereas the β-positive cells induced by CDDP displayed evidently enlarged morphology, the β-positive cells induced by Vem or Dab only displayed a mild increase in cellular morphology (Fig. 2A). Similar change of cellular morphology was observed in senescent A375 cells induced by one dose of Vem (Supplementary Figure S1-S2). The results implied that different mechanisms were employed to induce cell senescence in BRAFi- and CDDP-treated cells.

3.3. One dose of vem induces senescence-like cells in $BRAF^{V600E}$ melanoma cells

To exclude the direct effect of Vem on β-gal activity, one single dose of Vem was added into the culture medium and removed after 3 days, and β-gal staining was performed after another 2 or 5 days (Fig. 3A). The results demonstrated that Vem (0.5 μM–20 μM) could also evidently enhance β-gal staining in A375 cells. The blue color depth increased with culture duration and Vem concentration (Supplementary Fig. S1). Vem at 10 μM or higher concentration induced most of the A375 cells into blue-stained cells by day 5 and day 8 (Fig. 3B). Similarly, in melanoma M14 and A875 cells, 10 μM of Vem induced most of the cells into β-gal positive (Fig. 3C and D). Therefore, one dose of Vem at 10 μM was used to explore the cell senescence phenotype in subsequent experiments.

Cell cycle arrest is a fundamental characteristic of cell senescence. Proliferation inhibition was preliminarily observed in melanoma cells treated with Vem, Dab, or CDDP. To evaluate cell proliferation more precisely, an EdU integration assay was performed on day 5 after one single treatment with Vem (10 μM) or CDDP (2 μM) (Fig. 3A). The results demonstrated that the ratios of EdU integration declined significantly in both treatments and suggested that most of the remaining cells entered into cell cycle arrest and were authentic senescent cells (Fig. 3E and F).

3.4. Senescence-like cells induced by vem treatment do not enter apoptosis

Cell apoptosis is a frequent destiny in stressed cells. To evaluate the possibility of cell apoptosis in Vem-treated cells, mitochondrial membrane potential was detected using a JC-1 probe. The results showed that one dose of Vem treatment did not evidently induce the production of JC-1 monomers in $BRAF^{V600E}$ melanoma cells, based on the low intensity of green fluorescence (Supplementary Fig. S2). By contrast, CDDP treatment increased green fluorescence while decreasing red fluorescence in some cells, indicating the decline of mitochondrial membrane potential and the early stage of apoptosis. The results suggest that the adherent cells after Vem treatment did not enter apoptosis.

3.5. Vem-induced cell senescence is related to cyclin D1/p-Rb pathway inhibition

To explore the possible mechanisms underpinning Vem-induced cell senescence, signal pathways related to cell senescence or proliferation were detected. Senescent cells induced by a single treatment with Vem or CDDP were harvested on day 5, as shown in Fig. 3A. Consistent with our previous report [7], DNA damage-mediated activation of p53/p21 pathway was observed in the senescent cells induced by CDDP (SenC). However, in the senescent cells induced by Vem (SenV), neither DNA damage marker γ-H2AX nor p53/p21 pathway was evidently activated in A375, M14, and A875 cells, except for a mild upregulation of p21 in A875 cells (Fig. 4A). Therefore, the results excluded the substantial involvement of the DNA damage/p53/p21 pathway in Vem-induced senescence.

The tumor suppressor retinoblastoma protein (Rb) plays an important role in cell senescence [13]; its activity is regulated by p16 and cyclin D1. In this study, we observed the downregulation of p-Rb and/or cyclin D1 in the SenV of the three $BRAF^{V600E}$ cell lines (Fig. 4A). The expression of p16 did not show an obvious change, which might be attributed to the inactivation of the CDKN2A (p16) gene in melanoma cell lines [14]. Notably, Vem rapidly inhibited the cyclin D1/p-Rb pathway as early as 12 h after treatment (Fig. 4B–D). The results suggest that the suppression of cyclin D1/p-Rb occurred earlier than cell senescence and might be a key mechanism in Vem-induced senescence.

Interestingly, although Vem had been removed 2 days earlier, *p*-ERK1/2 level was still suppressed in SenV of A375 and M14 cells (Fig. 4A). However, in SenC, *p*-ERK1/2 was steadily elevated. Regarding AKT pathway, which is related to cell proliferation and Vem

resistance [15,16], the active *p*-AKT was robustly enhanced in SenV while only moderately elevated in SenC (Fig. 4A). Actually, Vem could enhance *p*-AKT levels after 12-h treatment in the A375 and M14 cells (Fig. 4B and C). Nevertheless, it is still to determine whether the suppressed ERK1/2 and activated AKT pathways are the inherent features of Vem-induced senescence.

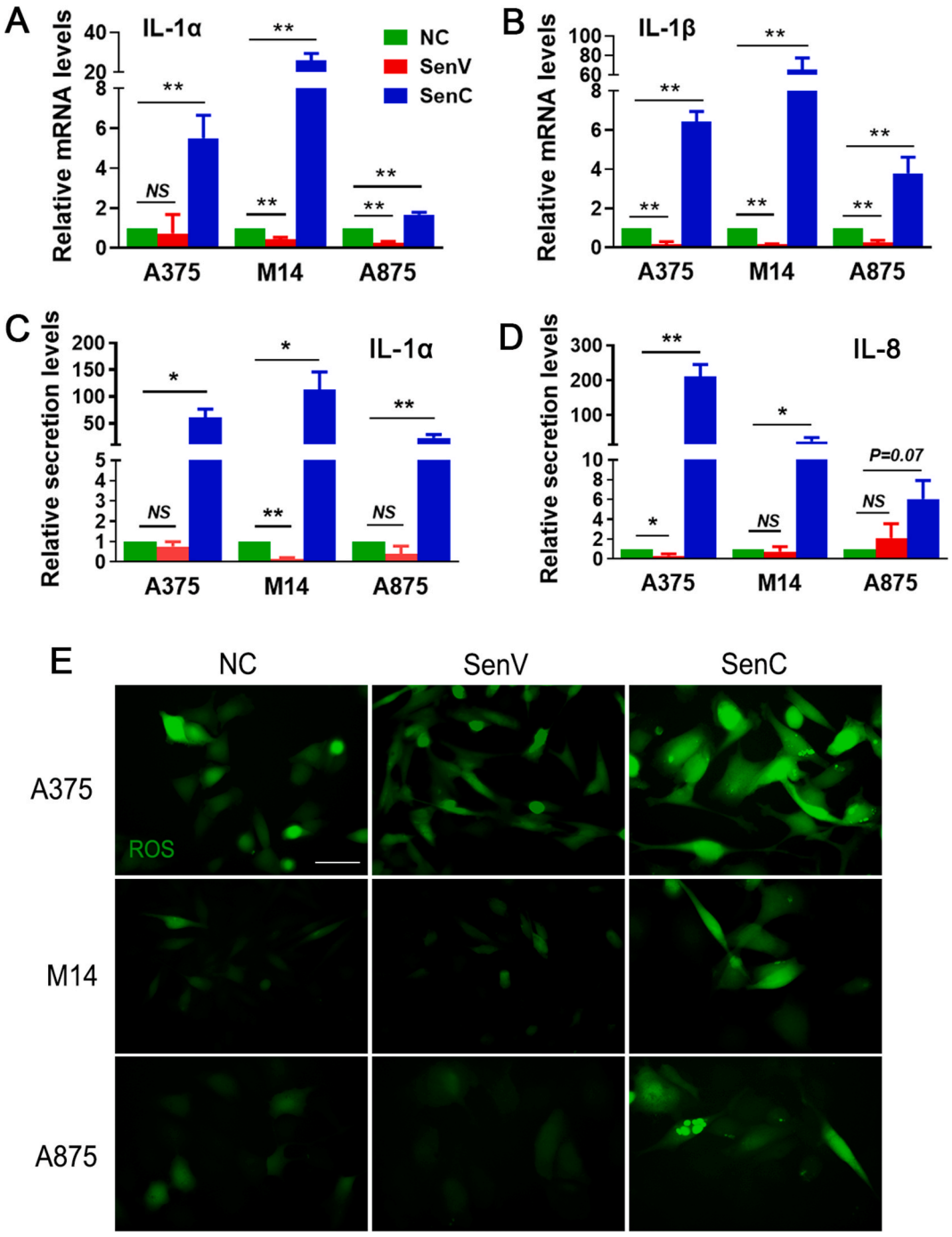

Fig. 5. SenV and SenC display different SASP and ROS levels.
The senescent cells induced by Vem or CDDP were obtained as shown in Fig. 3A. (A–B) The mRNA levels of classical SASP cytokines IL-1α, IL-1β in SenV and SenC detected by quantitative RT-PCR. (*C*-D) The protein secretion levels of SASP cytokines IL-1α and IL-8 detected by ELISA. (E) A DCFH-DA probe was used to evaluate ROS levels based on the intensity of green fluorescence. SenC displayed the strongest fluorescence, whereas SenV had the weakest signal among SenC, SenV, and NC. Bar is 50 μm. *NS*, significant; $^{*}P < 0.05$, $^{**}P < 0.01$ *vs.* NC (n = 3).

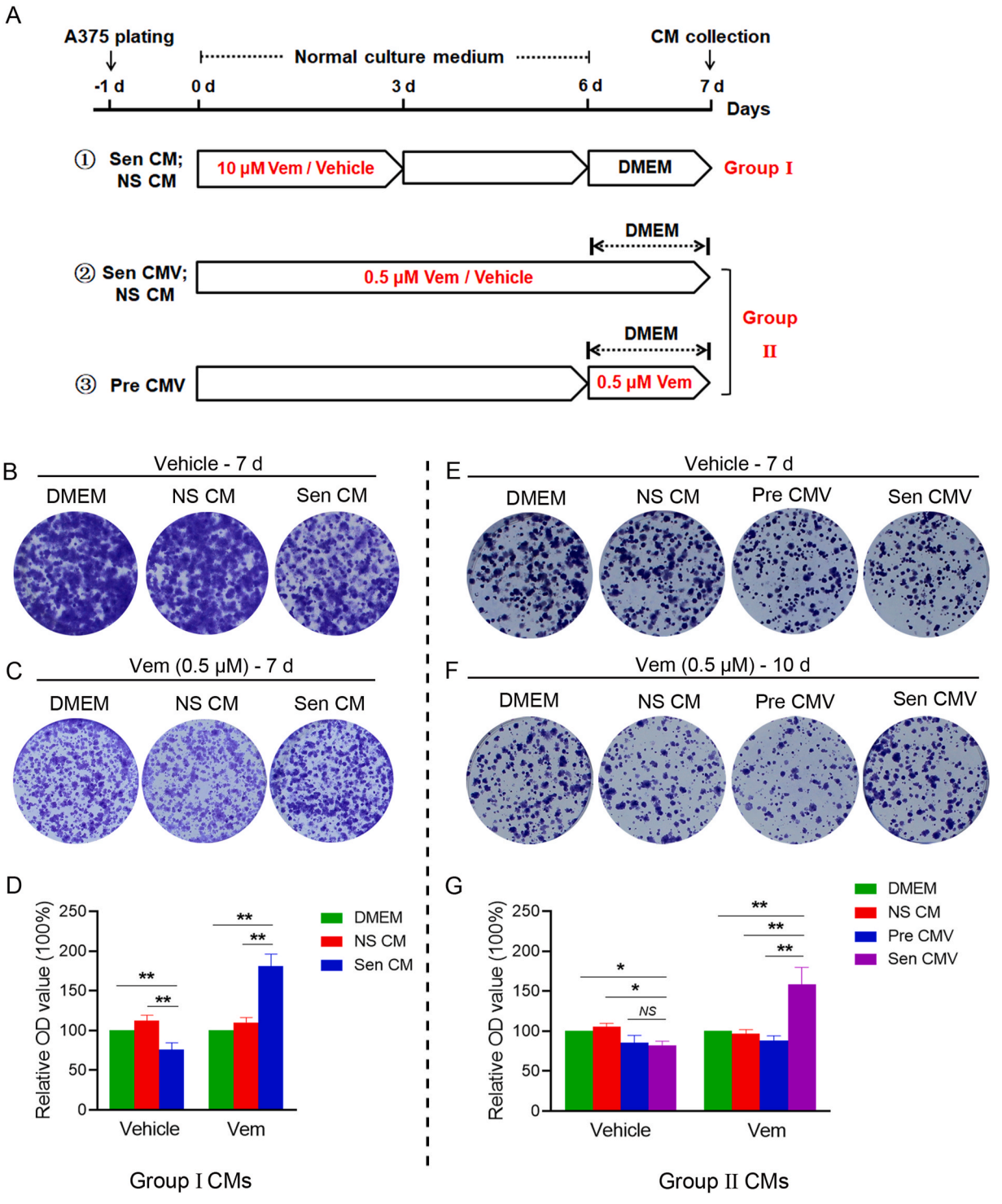

(caption on next page)

Fig. 6. Conditioned medium (CM) of senescent A375 cells exerts a resistant effect on Vem evaluated by clone formation assay.
(A) Two groups of senescent CM (Sen CM), together with control CM, were collected after treating A375 cells with one dose or continuous Vem administration and referred to as group I and group II CMs, respectively. The senescent and pre-senescent CM in group II contained residual Vem and were defined as Sen CMV and Pre CMV, respectively. Non-senescent CM (NS CM) and Pre CMV were control CM. Fresh DMEM medium with or without Vem was used before CM collection. (B–G) Exploring the effect of Sen CM or Sen CMV on cell proliferation and Vem resistance. The various CMs were diluted 1:1 with fresh DMEM before use. A375 cells were cultured in the diluted CMs plus 10% FBS, and Vem was continuously added up to the indicated concentration. The same volume of DMEM, NS CM, or Pre CMV acted as the control. (B–C, *E*-F) Representative clones showing the effect of Sen CM or Sen CMV on cell proliferation and Vem resistance. (D, G) Relative OD values of crystal violet. The cells in different rows might be stained at different times due to the differential growth rate. Horizontal comparison revealed an evident resistance of Sen CM or Sen CMV to Vem. *P < 0.05, **P < 0.01 (n $= 3$). NS means not significant.

3.6. Vem-induced senescent cells do not display a classical senescence-associated secretory phenotype

SASP is a frequent phenotype of senescent cells. To explore whether SenV had SASP similar to that of SenC, the expression levels of some classical SASP cytokines were detected. Consistent with our reports [7], the IL-1α and IL-1β mRNA were dramatically upregulated in the SenC of A375, M14, and A875 cells. However, the two genes were generally downregulated in SenV, compared with the negative control (Fig. 5A and B). ELISA confirmed that the secretion levels of IL-1α and IL-8, another classical SASP factor, displayed a decrease tendency in SenV while being dramatically elevated in SenC (Fig. 5C and D). The results suggest that classical SASP cytokines were suppressed in SenV.

ROS accumulation reportedly participates in the occurrence of classical SASP [17,18]. To account for the possible reasons underpinning the different SASP between SenV and SenC, the expression levels of ROS were detected using a DCFH-DA probe. Consistently, whereas green fluorescence increased in SenC, which implied ROS accumulation, the fluorescence intensity mildly reduced in SenV compared with the control group (Fig. 5E). The results suggest that the differential ROS levels may partially account for the differential SASP.

3.7. The culture supernatant of SenV displays resistance to vem

Although SenV did not produce typical SASP cytokines, it might still secrete other cytokines to affect Vem sensitivity. To explore the possible effect of the SenV culture supernatant on Vem resistance, two groups of CM were harvested from senescent A375 cells. In one group, a single Vem (10 μM) treatment was used to obtain Vem-free senescent CM (Sen CM). Non-senescent CM (NS CM) was simultaneously collected by using the vehicle instead of Vem (Fig. 6A). In another group, continuous Vem (0.5 μM) treatment, mimicking clinical practice, was used to obtain Vem-containing Sen CM (Sen CMV). A pre-senescent CM containing Vem (Pre CMV) was also prepared as control by treating cells with Vem for 24 h before CM collection (Fig. 6A).

The various CMs were mixed with DMEM medium (1:1) and used in the clone formation assay of A375 cells. The results showed that in Vem-free conditions, Sen CM weakly inhibited cell proliferation compared with DMEM and NS CM. However, in the Vem-containing medium, the Sen CM group displayed the strongest proliferation among the three groups (Fig. 6B–D). For the Vem-containing CMs, both Sen CMV and Pre CMV similarly inhibited A375 cell proliferation in the Vem-free conditions compared with DMEM and NS CM. However, in the presence of Vem, the cells in Sen CMV demonstrated the strongest proliferation (Fig. 6E–G). These results suggest that the Vem-induced senescent CMs contained cytokines that conferred resistance against Vem.

To address whether the senescent CMs of M14 and A875 cells also displayed similar resistance, Sen CM and Pre CM were prepared by treating the cells continuously with Vem for 6 days and 1 day, respectively. The cells were then incubated with DMEM medium for 24 h before the CMs collection (Supplementary Fig. S3A). In the clone formation assay of M14 and A875 cells, neither Sen CM nor Pre CM affected cell proliferation in the Vem-free condition. However, in the Vem-containing condition, the cells cultured in Sen CM displayed the strongest proliferation compared to the cells cultured in DMEM, NS CM, or Pre CM (Supplementary Fig. S3B–E). The results confirmed a resistant effect of the Sen CM of the M14 and A875 cells.

3.8. Screening of vem-resistant cytokines in senescent CM

To identify the exact SASP cytokines released from SenV, which underpinned Vem resistance, A375 cells of SenV, SenC, and the negative control (NC) were collected for RNA-seq. The differentially expressed genes (DEGs) of SenV/NC and SenC/NC were pooled and analyzed. Consistent with Western blot results, gene set enrichment analysis (GSEA) showed that the p53 pathway gene set was enriched in SenC but not in SenV (Supplementary Fig. S4). Kyoto Encyclopedia of Genes and Genomes (KEGG) enrichment demonstrated that the DEGs of SenV/NC and SenC/NC were pooled into different pathways. Venn analysis combined with the Reactome pathway revealed that interferon signaling was enriched in the overlapped up-regulation genes of SenV/NC and SenC/NC, while the cell cycle pathway was enriched in the overlapped down-regulation genes. Genes uniquely upregulated in SenV/NC were enriched in glycosylation-related pathways. (Supplementary Fig. S5–S9).

Since Vem and CDDP employed different mechanisms to induce cell senescence and displayed different SASP, we proposed that the Vem-resistant cytokines should be specifically elevated in SenV. Based on this hypothesis, we collected the DEGs—that is, genes in the sets SenV/NC ≥ 1.5, SenV/SenC≥ 1.5, and SenC/NC ≤ 2. Among these DEGs, 33 extracellular cytokines were obtained based on GO cellular component analysis (GO: 0005576) [19] (Fig. 7A). From the 33 cytokines specifically upregulated in SenV, three candidate genes—tissue inhibitor metalloproteinase 2 (TIMP2), *C*–C motif ligand 2 (CCL2), and nerve growth factor receptor (NGFR)—were

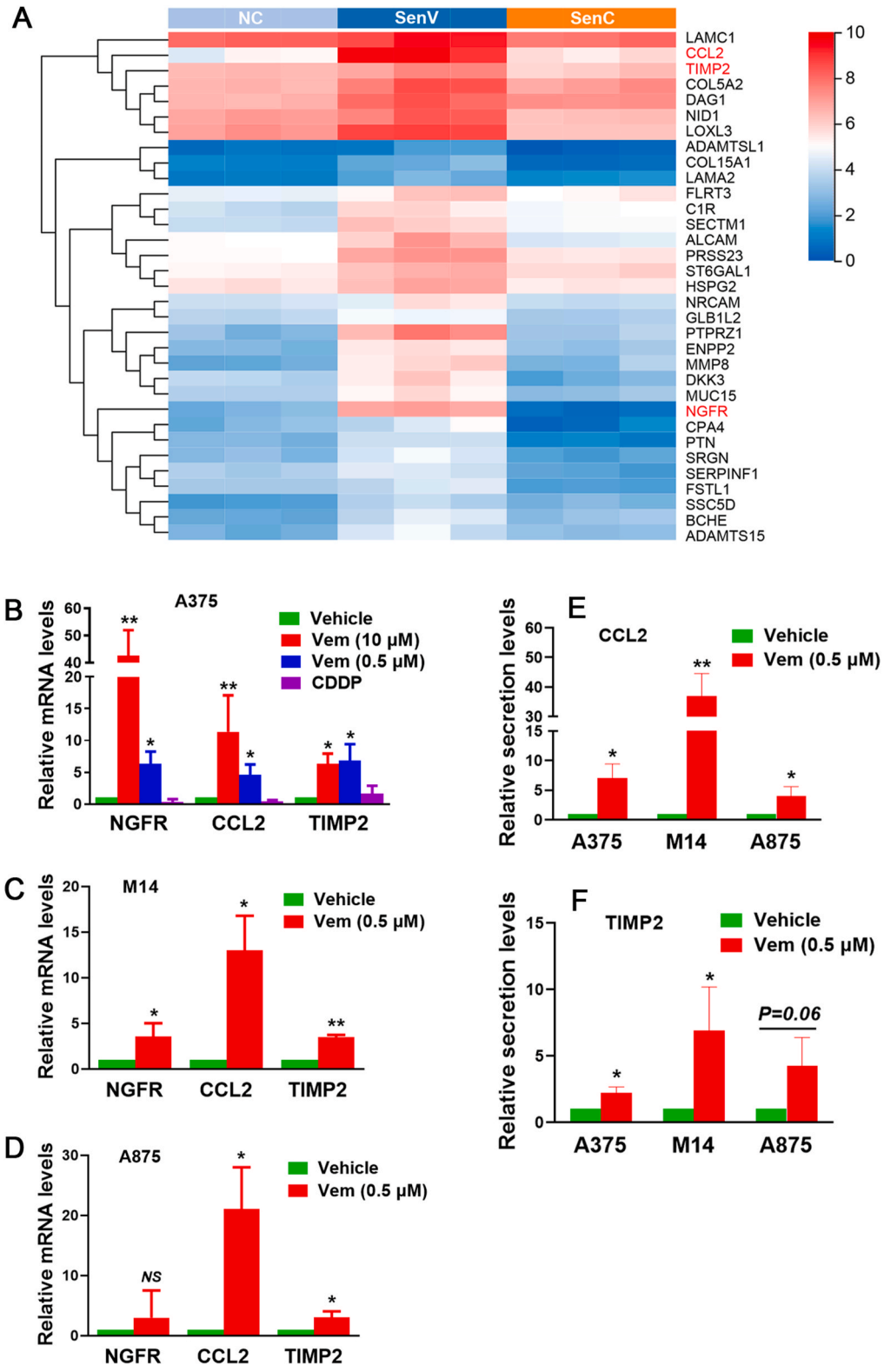

Fig. 7. Exploring the SASP cytokines uniquely high-expressed in SenV.
(A) The expression heatmap of cytokine genes, which showed the highest expression in SenV compared to NC and SenC. Cell senescence was induced by treating cells once with Vem (10 μM) or CDDP (2 μM) and RNA-seq was performed on day 7 after treatment. CCL2, TIMP2, and NGFR were chosen for further verification. (B) The relative mRNA levels of NGFR, CCL2, and TIMP2 in senescent A375 cells induced by a single treatment

with Vem (10 μM), continuous treatment with Vem (0.5 μM), or single treatment with CDDP (2 μM). (C–D) Relative mRNA levels of NGFR, CCL2, and TIMP2 in senescent M14 and A875 cells induced by continuous Vem treatment. (E–F) The relative secretion levels of CCL2 and TIMP2 in Sen CM induced by continuous Vem treatment, evaluated by ELISA. *P < 0.05, **P < 0.01 vs. Vehicle (n = 3). NS means not significant.

chosen for further investigation based on their involvement in the MAPK pathway [20–22]. qRT-PCR confirmed that TIMP2, CCL2, and NGFR were upregulated in senescent A375 cells induced by either single or continuous treatments with Vem (Fig. 7B). Upregulation of the three cytokines was also observed in senescent M14 and A875 cells induced by continuous Vem treatment (Fig. 7C and D). To confirm the secretion of cytokines into the supernatant, TIMP2 and CCL2 were chosen for ELISA detection. The results verified that TIMP2 and CCL2 secretion were dramatically enhanced in the SenV supernatant of A375, M14, and A875 cells (Fig. 7E and F).

Next, we investigated the effects of TIMP2, CCL2, and NGFR on cell proliferation and Vem resistance using a clone formation assay. The results showed that in the Vem-free medium, the three cytokines exerted negligible or weak effects on cell proliferation, but in the Vem-containing medium, the cytokines generally attenuated the inhibitory effect of Vem on cell proliferation (Fig. 8). These results indicate that TIMP2, CCL2, and NGFR were among the SASP cytokines of SenV that promoted Vem resistance.

3.9. *Vem treatment induces melanoma cells into senescence in vivo*

To evaluate whether Vem could induce cell senescence in vivo, melanoma-bearing mice were established by subcutaneous injection of A375 cells into nude mouse. Vem or vehicle gavage was performed when the average tumor volume reached about 150 mm^3. Seven days after the treatment, tumor tissues were collected for detection. Compared with vehicle treatment, Vem evidently inhibited tumor growth. β-Gal staining showed that the Vem-treated tumor slices contained more blue-stained foci than the vehicle-treated ones. Western blot analysis showed that Vem-treated tumor tissues displayed suppressed expression of *p*-ERK1/2, which demonstrated the effectiveness of Vem (Fig. 9). However, cyclin D1 and p-Rb levels displayed no evident difference between Vem- and vehicle-treated tissues (data not shown), which might be ascribed to the cell heterogeneity of tumor tissues and the lower percentage of β-gal-positive cells in vivo.

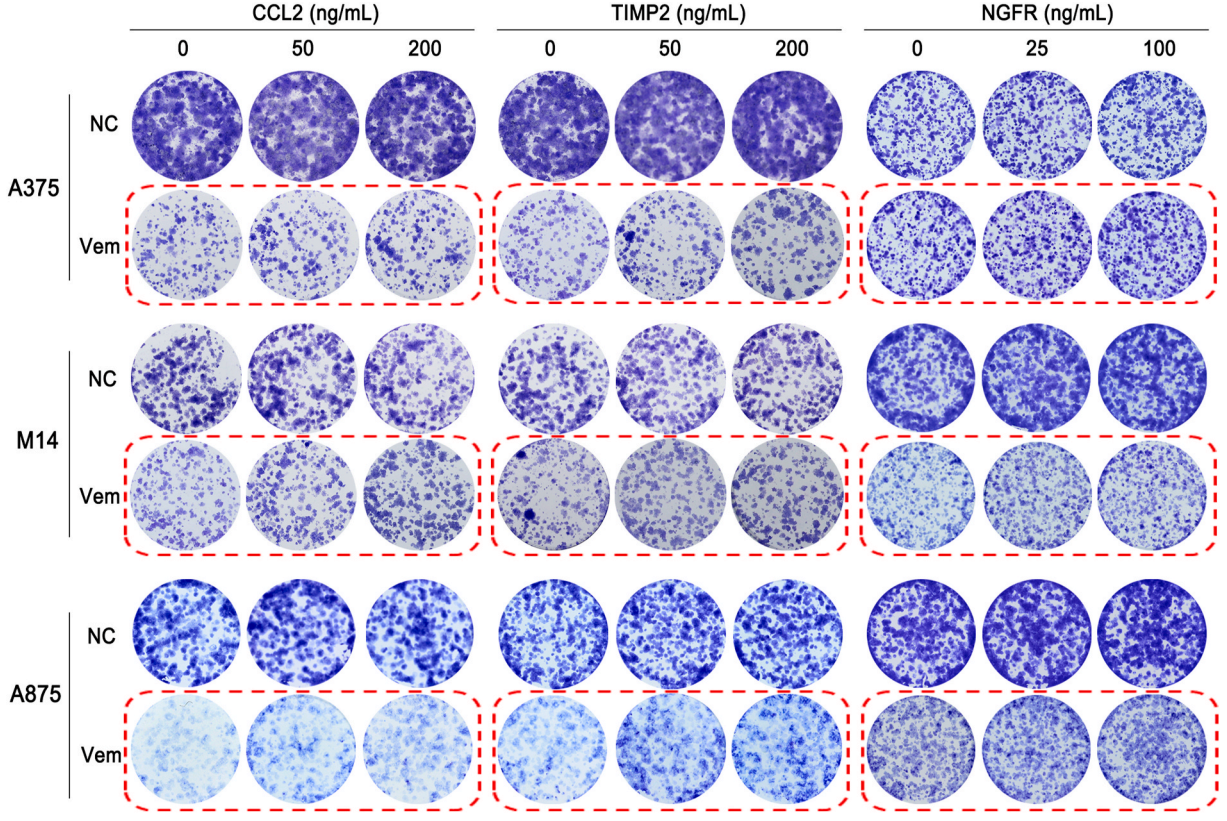

Fig. 8. The cytokines CCL2, TIMP2, and NGFR display resistance to Vem.
CCL2, TIMP2, and NGFR were diluted and added into 10% FBS culture medium with or without Vem. The effects of these cytokines on cell proliferation and Vem sensitivity were evaluated by clone formation. When obvious clones could be observed, the cells were fixed and stained. Due to different growth rates, the NC and Vem groups might be stained at different times. Horizontal comparison revealed that these cytokines alone had negligible or weak effects on cell proliferation, but they generally displayed resistance to Vem. Similar results were observed in 3 independent experiments. The red quadrangles contain the control and experiment groups to facilitate comparison.>

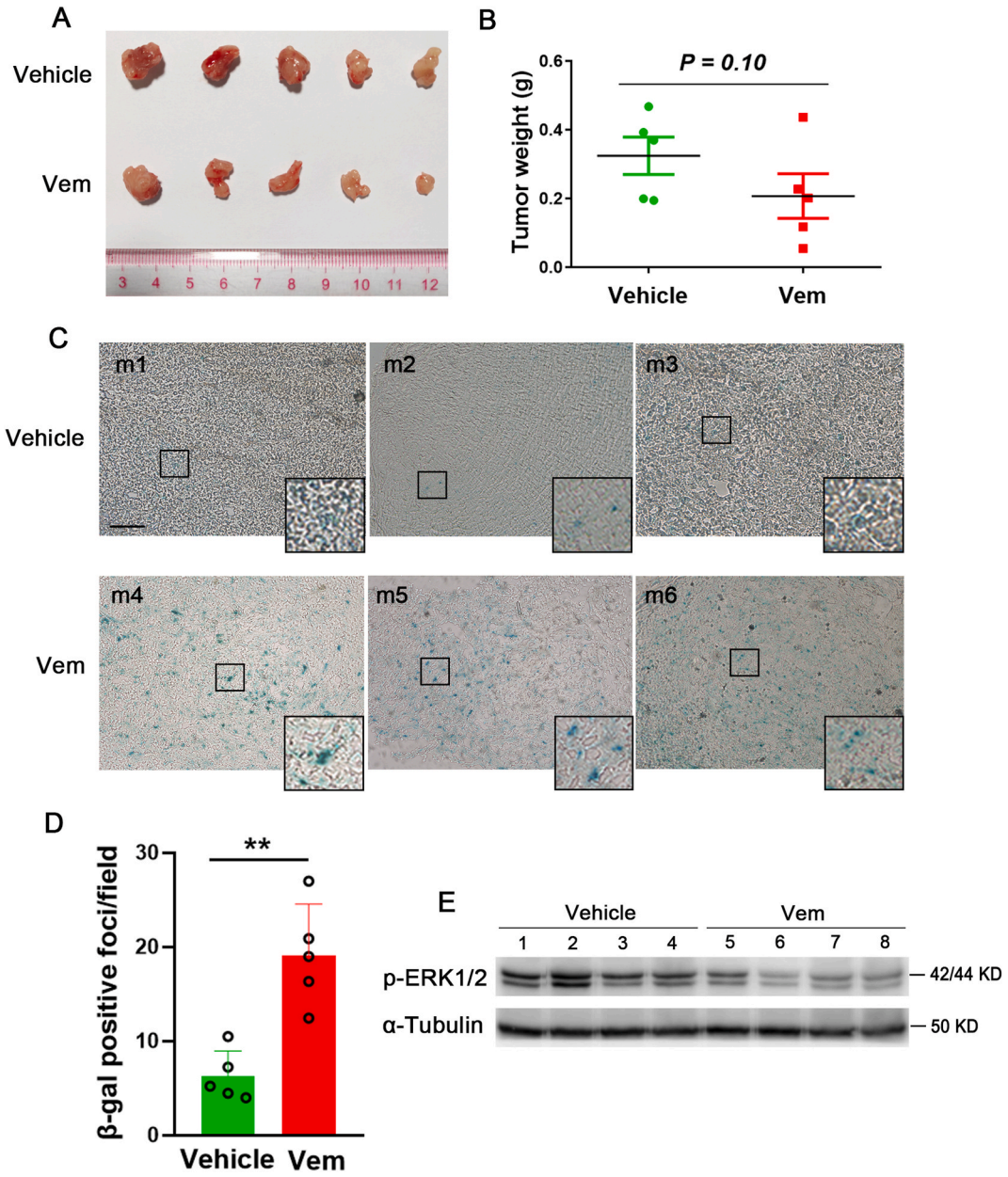

Fig. 9. Vem induces melanoma cells into β-gal-positive in vivo.
Tumor-bearing mice were established by subcutaneous injection with melanoma A375 cells. When obvious tumor masses were observed, Vem gavage was performed daily for 7 days. The tumor tissues were then detected. (A) The melanoma tissues after 7-day treatment with Vem or vehicle. (B) Tumor weights of Vem- and vehicle-treated mice (n = 5). (C) Representative β-gal staining of tumor slices. Each picture represents a typical staining in one mouse. (D) The number of β-gal positive foci per field in Vem- and vehicle-treated tumor tissues. (E) Expression levels of *p*-ERK1/2 in Vem- and vehicle-treated tumor lysates. Bar is 100 μM $^{**}P < 0.01$ (n = 5).

4. Discussion

Reactivation of BRAF/MEK and compensatory activation of PI3K/AKT pathways are the key mechanisms which lead to BRAFi resistance as well as cross-resistance to other medication [4,15,16]. The adaptive response of melanoma or the tumor microenvironment also plays important roles in BRAFi resistance [19,23]. Researchers suggested that melanoma cell senescence is an adaptive response to treatment [7,10]. In this study, Vem induced evident cell senescence in $BRAF^{V600E}$ melanoma cells, manifested by β-gal staining, mildly enlarged cell morphology, cell cycle arrest, and inhibition of the cyclin D1/p-RB pathway. These phenotypes are generally consistent with other reports of senescent melanoma cells [8,9]. Downregulation of Cyclin D1/p-Rb would result in Rb

activation, which might underpin the Vem-induced senescence based on the key role of Rb in cell senescence [13].

BRAF is an oncogene that can provoke oncogene-induced senescence (OIS) in melanocytes [24]. Overcoming the barrier of OIS is a prerequisite for melanomagenesis [25–27]. It was interesting to find that melanoma cells that had overcome OIS restored senescence after BRAF inhibition. Although SenV had different phenotypes compared with those of OIS [28,29], they might share similar mechanisms to induce cell senescence. Increased mitochondrial oxidative metabolism is the key mechanism underlying OIS [24], while $BRAF^{V600E}$ melanoma has increased glycolysis [30]. This discrepancy implies a metabolism shift from oxidative metabolism to glycolysis during melanomagenesis. Vem can suppress glycolysis and enhance oxidative metabolism [31], which implies a recapitulation of OIS in Vem-treated cells. Based on this hypothesis, it is no wonder that the BRAF-mutant melanoma cells entered senescence more easily than the wild-type ones.

The senescent cells induced by Vem also showed some specific phenotypes. The SenV did not display the activation of DNA damage/p53/p21 pathway, accumulation of ROS, and enhanced expression of traditional SASP cytokines, most of which are obvious in senescent cells induced by CDDP or other stressors [10,13,29]. In fact, SenV displayed a suppression of classical SASP cytokines. A persistent DNA damage response and ROS accumulation are known to be necessary for traditional SASP [17,32]. In this study, the mild suppression of ROS levels in SenV might partially account for the inhibition of canonical SASP cytokines. Some canonical SASP cytokines, such as IL-8 and TGF-β, are the downstream effectors of BRAF-ERK1/2 pathway and thus can be inhibited by BRAFi [8]. In this study, Vem was washed out several days before SASP detection, which mostly excluded its direct effect and suggested that the suppression of traditional SASP might be a unique characteristic of Vem-induced senescence.

Despite the inhibition of canonical SASP cytokines, SenV displayed enhanced expression and secretion of some cytokines. In previous reports, the CM of SenC directly promoted the proliferation of normal melanoma cells [7]. In this study, the CM of SenV did not enhance the proliferation of melanoma cells, but it attenuated the inhibitory effect of Vem on cell proliferation. Among the SASP cytokines highly expressed in SenV, TIMP2, CCL2, and NGFR might be the key cytokines exerting resistance to Vem.

CCL2 can regulate or be regulated by the MAPK pathway [20,33]. CCL2 can also promote Vem resistance by inducing proliferation-related miRNAs [34]. BRAFi treatment initially decreases CCL2 expression [35], but increases it after long-term treatment [36]. The quick increase in CCL2 in SenV indicates the fast adaptive response of melanoma cells in vitro. TIMP-2 is an inhibitor of multiple metalloproteinases and can also activate MAPK pathway [21]. TIMP-2 protects melanoma cells from apoptosis by activating NF-κB pathway [37]. However, the exact mechanisms by which TIMP-2 resists Vem have yet to be investigated. NGFR belongs to the tumor necrosis factor receptor superfamily, which can activate MAPK and NF-κB pathways [22]. NGFR also plays an important role in melanoma metastasis [22] and is related to adaptive resistance and therapy resistance to BRAFi [38–40]. Besides the three cytokines, other cytokines among the 33 upregulated SASP cytokines, such as NID1 [41] and MMP8 [42], are also reportedly involved in melanoma proliferation or Vem resistance. Nevertheless, it should be kept in mind that in SenV, not all cells were senescent cells. Detecting the cytokines expression in single cell level would be necessary in further study.

5. Conclusions

Our findings indicate that Vem robustly induced $BRAF^{V600E}$ melanoma cells into senescence. The senescent cells displayed some distinct characteristics and secreted some non-classical SASP cytokines, which facilitated Vem resistance by supporting melanoma cells proliferation upon treatment. Targeting SASP cytokines with neutralizing antibodies or eliminating senescent cells with senolytics might be a potent strategy for overcoming Vem resistance in melanoma.

Funding

This work was supported by National Natural Science Foundation of China (81971329), Natural Science Foundation of Guangdong Province (2021A1515012236, 2020A1515010026, 2019A1515010261), Special Correspondent Project of Dongguan City (20201800500042), Cultivation Funds of Guangdong Medical University (GDMUZ2020007), Competitive Funds of Zhanjiang Science and Technology Development (2020A01033), Teaching Reform Project of Guangdong Medical University (1JG21087), Discipline Construction Project of Guangdong Medical University (4SG23287G, 4SG21008G) and Medical Scientific Research Fund of Guangdong Province (A2023494).

Ethics statement

The research was done following the guidelines for the Animal Ethics Committee of Guangdong Medical University (Approval No. GDY1902028).

Author contribution statement

Jianyu Peng: Conceived and designed the experiments; Performed the experiments; Wrote the paper.
Zijun Lin; Lin Yao; Minla Rao: Performed the experiments.
Weichun Chen: Conceived and designed the experiments.
Jie Ruan; Fan Deng; Xingdong Xiong; Shun Xu: Analyzed and interpreted the data.
Xiangning Zhang: Contributed reagents, materials, analysis tools or data.
Xinguang Liu: Conceived and designed the experiments; Contributed reagents, materials, analysis tools or data.

Xuerong Sun: Conceived and designed the experiments; Contributed reagents, materials, analysis tools or data; Wrote the paper.

Data availability statement

Data associated with this study the RNA-seq data have been deposited in NCBI's Gene Expression Omnibus and can be accessed using GEO Series accession number GSE209769.

Declaration of competing Interest

The authors declare that they have no known competing financial interests or personal relationships that could have appeared to influence the work reported in this paper.

Appendix A. Supplementary data

Supplementary data to this article can be found online at https://doi.org/10.1016/j.heliyon.2023.e17714.

References

[1] T. Krishnan, A.M. Menzies, R. Roberts-Thomson, Recent advancements in melanoma management, Intern. Med. J. 51 (3) (2021) 327–333.
[2] B.D. Curti, M.B. Faries, Recent advances in the treatment of melanoma, N. Engl. J. Med. 384 (23) (2021) 2229–2240.
[3] A.M. Schmitt, L. Dumas, J. Larkin, Atezolizumab, cobimetinib, and vemurafenib as first-line treatment for unresectable metastatic BRAF V600 mutated melanoma, Expet Rev. Anticancer Ther. 22 (1) (2022) 17–25.
[4] A.M. Czarnecka, E. Bartnik, M. Fiedorowicz, P. Rutkowski, Targeted therapy in melanoma and mechanisms of resistance, Int. J. Mol. Sci. 21 (13) (2020).
[5] J. Jandova, G.T. Wondrak, Vemurafenib drives epithelial-to-mesenchymal transition gene expression in BRAF inhibitor–resistant BRAF(V600E)/NRAS(Q61K) melanoma enhancing tumor growth and metastasis in a bioluminescent murine model, J. Invest. Dermatol. 142 (5) (2022) 1456–1465.e1451.
[6] F. Ahmed, H.-Y. Tseng, A. Ahn, D. Gunatilake, S. Alavi, M. Eccles, H. Rizos, S.J. Gallagher, J.C. Tiffen, P. Hersey, Repurposing melanoma chemotherapy to activate inflammasomes in the treatment of BRAF/MAPK inhibitor resistant melanoma, J. Invest. Dermatol. 142 (5) (2022) 1444–1455.
[7] X. Sun, B. Shi, H. Zheng, L. Min, J. Yang, X. Li, X. Liao, W. Huang, M. Zhang, S. Xu, et al., Senescence-associated secretory factors induced by cisplatin in melanoma cells promote non-senescent melanoma cell growth through activation of the ERK1/2-RSK1 pathway, Cell Death Dis. 9 (3) (2018) 260.
[8] M. Krayem, A. Najem, F. Journe, R. Morandini, F. Sales, A. Awada, G.E. Ghanem, Acquired resistance to BRAFi reverses senescence-like phenotype in mutant BRAF melanoma, Oncotarget 9 (61) (2018) 31888–31903.
[9] S. Haferkamp, A. Borst, C. Adam, T.M. Becker, S. Motschenbacher, S. Windhövel, A.L. Hufnagel, R. Houben, S. Meierjohann, Vemurafenib induces senescence features in melanoma cells, J. Invest. Dermatol. 133 (6) (2013) 1601–1609.
[10] M.R. Webster, M. Xu, K.A. Kinzler, A. Kaur, J. Appleton, M.P. O'Connell, K. Marchbank, A. Valiga, V.M. Dang, M. Perego, et al., Wnt5A promotes an adaptive, senescent-like stress response, while continuing to drive invasion in melanoma cells, Pigment Cell Melanoma Res 28 (2) (2015) 184–195.
[11] M. Rao, B. Shi, Y. Yuan, Y. Wang, Y. Chen, X. Liu, X. Li, M. Zhang, X. Liu, X. Sun, The positive correlation between drug addiction and drug dosage in vemurafenib-resistant melanoma cells is underpinned by activation of ERK1/2-FRA-1 pathway, Anti Cancer Drugs 31 (10) (2020) 1026–1037.
[12] R. Edgar, M. Domrachev, A.E. Lash, Gene Expression Omnibus: NCBI gene expression and hybridization array data repository, Nucleic Acids Res. 30 (1) (2002) 207–210.
[13] R. Di Micco, V. Krizhanovsky, D. Baker, F. d'Adda di Fagagna, Cellular senescence in ageing: from mechanisms to therapeutic opportunities, Nat. Rev. Mol. Cell Biol. 22 (2) (2021) 75–95.
[14] M. Castellano, P.M. Pollock, M.K. Walters, L.E. Sparrow, L.M. Down, B.G. Gabrielli, P.G. Parsons, N.K. Hayward, CDKN2A/p16 is inactivated in most melanoma cell lines, Cancer Res. 57 (21) (1997) 4868–4875.
[15] M. Radić, I. Vlašić, M. Jazvinšćak Jembrek, A. Horvat, A. Tadijan, M. Sabol, M. Dužević, M. Herak Bosnar, N. Slade, Characterization of vemurafenib-resistant melanoma cell lines reveals novel hallmarks of targeted therapy resistance, Int. J. Mol. Sci. 23 (17) (2022).
[16] S. Erdmann, D. Seidel, H.G. Jahnke, M. Eichler, J.C. Simon, A.A. Robitzki, Induced cross-resistance of BRAF(V600E) melanoma cells to standard chemotherapeutic dacarbazine after chronic PLX4032 treatment, Sci. Rep. 9 (1) (2019) 30.
[17] G. Nelson, O. Kucheryavenko, J. Wordsworth, T. von Zglinicki, The senescent bystander effect is caused by ROS-activated NF-κB signalling, Mech. Ageing Dev. 170 (2018) 30–36.
[18] H.J. Kim, W.J. Kim, H.R. Shin, H.I. Yoon, J.I. Moon, E. Lee, J.M. Lim, Y.D. Cho, M.H. Lee, H.G. Kim, et al., ROS-induced PADI2 downregulation accelerates cellular senescence via the stimulation of SASP production and NFkappaB activation, Cell. Mol. Life Sci. 79 (3) (2022) 155.
[19] A.C. Obenauf, Y. Zou, A.L. Ji, S. Vanharanta, W. Shu, H. Shi, X. Kong, M.C. Bosenberg, T. Wiesner, N. Rosen, et al., Therapy-induced tumour secretomes promote resistance and tumour progression, Nature 520 (7547) (2015) 368–372.
[20] H. Yasui, H. Kajiyama, S. Tamauchi, S. Suzuki, Y. Peng, N. Yoshikawa, M. Sugiyama, K. Nakamura, F. Kikkawa, CCL2 secreted from cancer-associated mesothelial cells promotes peritoneal metastasis of ovarian cancer cells through the P38-MAPK pathway, Clin. Exp. Metastasis 37 (1) (2020) 145–158.
[21] G. Zhang, X. Luo, Z. Wang, J. Xu, W. Zhang, E. Chen, Q. Meng, D. Wang, X. Huang, W. Zhou, et al., TIMP-2 regulates 5-Fu resistance via the ERK/MAPK signaling pathway in colorectal cancer, Aging (Albany NY) 14 (1) (2022) 297–315.
[22] S. García-Silva, A. Benito-Martín, L. Nogués, A. Hernández-Barranco, M.S. Mazariegos, V. Santos, M. Hergueta-Redondo, P. Ximénez-Embún, R.P. Kataru, A. A. Lopez, et al., Melanoma-derived small extracellular vesicles induce lymphangiogenesis and metastasis through an NGFR-dependent mechanism, Nat. Can. (Que.) 2 (12) (2021) 1387–1405.
[23] H.L. Young, E.J. Rowling, M. Bugatti, E. Giurisato, N. Luheshi, I. Arozarena, J.C. Acosta, J. Kamarashev, D.T. Frederick, Z.A. Cooper, et al., An adaptive signaling network in melanoma inflammatory niches confers tolerance to MAPK signaling inhibition, J. Exp. Med. 214 (6) (2017) 1691–1710.
[24] J. Kaplon, L. Zheng, K. Meissl, B. Chaneton, V.A. Selivanov, G. Mackay, S.H. van der Burg, E.M. Verdegaal, M. Cascante, T. Shlomi, et al., A key role for mitochondrial gatekeeper pyruvate dehydrogenase in oncogene-induced senescence, Nature 498 (7452) (2013) 109–112.
[25] Y. Yu, K. Schleich, B. Yue, S. Ji, P. Lohneis, K. Kemper, M.R. Silvis, N. Qutob, E. van Rooijen, M. Werner-Klein, et al., Targeting the senescence-overriding cooperative activity of structurally unrelated H3K9 demethylases in melanoma, Cancer Cell 33 (4) (2018) 785.
[26] E.C. Canedo, S.D. Rincon, P. Siegel, M. Witcher, J. Ursini-Siegel, Abstract 131: the role of p66ShcA in the melanoma oncogenesis process, Cancer Res. 82 (12_Supplement) (2022) 131.
[27] E.L. Thompson, J.J. Hu, L.J. Niedernhofer, The role of senescent cells in acquired drug resistance and secondary cancer in BRAFi-treated melanoma, Cancers 13 (9) (2021).
[28] L. Wang, L. Lankhorst, R. Bernards, Exploiting senescence for the treatment of cancer, Nat. Rev. Cancer 22 (6) (2022) 340–355.

[29] X.L. Liu, J. Ding, L.H. Meng, Oncogene-induced senescence: a double edged sword in cancer, Acta Pharmacol. Sin. 39 (10) (2018) 1553–1558.
[30] A. Avagliano, G. Fiume, A. Pelagalli, G. Sanità, M.R. Ruocco, S. Montagnani, A. Arcucci, Metabolic plasticity of melanoma cells and their crosstalk with tumor microenvironment, Front. Oncol. 10 (2020) 722.
[31] T. Delgado-Goni, M.F. Miniotis, S. Wantuch, H.G. Parkes, R. Marais, P. Workman, M.O. Leach, M. Beloueche-Babari, The BRAF inhibitor vemurafenib activates mitochondrial metabolism and inhibits hyperpolarized pyruvate-lactate exchange in BRAF-mutant human melanoma cells, Mol. Cancer Therapeut. 15 (12) (2016) 2987–2999.
[32] F. Rodier, J.P. Coppe, C.K. Patil, W.A. Hoeijmakers, D.P. Munoz, S.R. Raza, A. Freund, E. Campeau, A.R. Davalos, J. Campisi, Persistent DNA damage signalling triggers senescence-associated inflammatory cytokine secretion, Nat. Cell Biol. 11 (8) (2009) 973–979.
[33] T. Kasemsuk, S. Phuagkhaopong, R. Yubolphan, N. Rungreangplangkool, P. Vivithanaporn, Cadmium induces CCL2 production in glioblastoma cells via activation of MAPK, PI3K, and PKC pathways, J. Immunot. 17 (1) (2020) 186–193.
[34] E. Vergani, L. Di Guardo, M. Dugo, S. Rigoletto, G. Tragni, R. Ruggeri, F. Perrone, E. Tamborini, A. Gloghini, F. Arienti, et al., Overcoming melanoma resistance to vemurafenib by targeting CCL2-induced miR-34a, miR-100 and miR-125b, Oncotarget 7 (4) (2016) 4428–4441.
[35] D.A. Knight, S.F. Ngiow, M. Li, T. Parmenter, S. Mok, A. Cass, N.M. Haynes, K. Kinross, H. Yagita, R.C. Koya, et al., Host immunity contributes to the anti-melanoma activity of BRAF inhibitors, J. Clin. Invest. 123 (3) (2013) 1371–1381.
[36] S.M. Steinberg, T.B. Shabaneh, P. Zhang, V. Martyanov, Z. Li, B.T. Malik, T.A. Wood, A. Boni, A. Molodtsov, C.V. Angeles, et al., Myeloid cells that impair immunotherapy are restored in melanomas with acquired resistance to BRAF inhibitors, Cancer Res. 77 (7) (2017) 1599–1610.
[37] J. Sun, W.G. Stetler-Stevenson, Overexpression of tissue inhibitors of metalloproteinase 2 up-regulates NF-kappaB activity in melanoma cells, J. Mol. Signal. 4 (2009) 4.
[38] M.L. Hartman, M. Sztiller-Sikorska, A. Gajos-Michniewicz, M. Czyz, Dissecting mechanisms of melanoma resistance to BRAF and MEK inhibitors revealed genetic and non-genetic patient- and drug-specific alterations and remarkable phenotypic plasticity, Cells 9 (1) (2020).
[39] M. Fallahi-Sichani, V. Becker, B. Izar, G.J. Baker, J.R. Lin, S.A. Boswell, P. Shah, A. Rotem, L.A. Garraway, P.K. Sorger, Adaptive resistance of melanoma cells to RAF inhibition via reversible induction of a slowly dividing de-differentiated state, Mol. Syst. Biol. 13 (1) (2017) 905.
[40] J. Diener, L. Sommer, Reemergence of neural crest stem cell-like states in melanoma during disease progression and treatment, Stem Cells Transl. Med. 10 (4) (2021) 522–533.
[41] V. Paulitschke, O. Eichhoff, C. Gerner, P. Paulitschke, A. Bileck, T. Mohr, P.F. Cheng, A. Leitner, E. Guenova, I. Saulite, et al., Proteomic identification of a marker signature for MAPKi resistance in melanoma, EMBO J. 38 (15) (2019), e95874.
[42] B. Yuan, L. Lin, Z.Y. Ying, M.X. Ying, Q.Y. Zhou, L. Shi, Repression of M-phase phosphoprotein 8 inhibits melanoma growth and metastasis in vitro and in vivo, Int. J. Clin. Exp. Pathol. 10 (12) (2017) 12003–12009.